

Is it Possible to Get a SAR Image of Ocean Waves Free of Spectral Cut-off by Direct Measurement?

Mikhail B. Kanevsky

Independent researcher, Canada

*Corresponding author

Mikhail B. Kanevsky, Independent researcher, Canada

Submitted: 08 Sept 2021; Accepted: 13 Sept 2021; Published: 20 Sept 2021

Citation: Mikhail Kanevsky (2021) Is it Possible to Get a SAR Image of Ocean Waves Free of Spectral Cut-off by Direct Measurement? *J Mari Scie Res Ocean*, 4(2): 228-231.

Abstract

A method of SAR sounding of the ocean surface is proposed, which is capable of providing an undistorted by spectral cut-off wave pattern. The method involves the use of two synchronized SARs, which look across the track line and illuminate the same area of the surface. Each SAR records its own backscattered signal, which are then multiplied with each other and the resulting signal is undergoing the procedure of matched filtering. Numerical estimates of the applicability conditions of the method are carried out.

Introduction

As is known, the main problem in interpreting images of the ocean surface formed by microwave synthetic aperture radar (SAR) is the distortions introduced by the orbital movements of the small-scale (centimeter and decimeter) ripples. The point is that the standard aperture synthesis procedure is a matched filtering operation aimed at extracting from the backscattered signal a part that has a phase that changes according to a known scenario corresponding to a stationary reflecting surface. The movement of the ripples responsible for microwave backscattering violates this scenario, which mainly manifests itself as cut-off of the high-frequency part of the image spectrum, which means a loss of azimuthal resolution and false indication of the direction of ocean wave propagation. The phenomenon of spectral cut-off was first pointed out in [1], and its physical meaning lies in the fact that, due to the motion of ripples in the field of large waves, images of various surface elements are randomly shifted and superimposed on each other [2-3].

Attempts to retrieve the wave spectrum from the SAR image have been undertaken by a number of authors (see [4], [5] and their references) using iterative algorithms that are based on the so-called modulation transfer function (MTF), which establishes the relationship between the spectral components of ocean roughness on the one hand and the radar cross section on the other. However, the possibility of creating a universal retrieval algorithm does not seem realistic, not only because of insufficient knowledge about MTF but also because of the many random factors modulating the intensity of ripples (surface manifestations of various interoceanic processes, pollution, fluctuations of the near-surface wind speed, etc.).

In this paper, we consider a method for directly obtaining the SAR image of ocean waves free of spectral cut-off, without using any a priori assumptions such as MTF. This method was previously proposed in the short communication [6], however, upon a deeper study of the issue, it turned out that it needs a more detailed justification.

Method Description

The proposed method involves the use of two synchronized SARs, which look across the track line and illuminate the same area of the surface (Figure. 1).

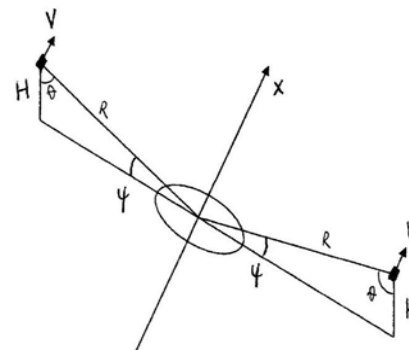


Figure 1: Probing geometry

Each SAR records its own backscattered signal, which are then multiplied with each other and the resulting signal is undergoing the procedure of matched filtering.

Recall that the standard aperture synthesizing operation is performed using the following transformation:

$$a_{\text{SAR}}(t) \propto \int_{t-\Delta t/2}^{t+\Delta t/2} dt' a(t') \exp \left[-i \frac{k}{R} V^2 (t' - t)^2 \right] \quad (1)$$

where a and a_{SAR} are, respectively, the complex amplitudes of the backscattered microwave electromagnetic field and the synthesized signal, the integration time Δt determines the nominal resolution of SAR. Besides, $k = 2\pi/\lambda$, where λ is the SAR working wavelength, R is the slant range (see Figure.1), and V is the SAR carrier speed.

Assuming the size of the SAR resolution cell in the ground range to be small in comparison with the characteristic wavelength on the surface, we will consider one row of the image in the azimuthal direction x . For the complex amplitude of the backscattered field, we write:

$$a(t') \propto \int_{\Delta x} dx' p(x', t') \exp \left[i \frac{k}{R} (x' - Vt')^2 \right] \quad (2)$$

where Δx is the azimuthal size of the physical resolution cell of the SAR, and $p(x', t')$ is the complex reflection coefficient of the surface.

Let the reflecting element of the surface be a point scatterer moving with a velocity, the radial component of which with respect to one of the SARs is v_{rad} , i.e.

$$p(x', t') = p_0 \delta(x' - x_0) \exp(-2ikv_{\text{rad}}t') \quad (3)$$

(Note that v_{rad} , the projection of the orbital velocity on the direction of the radar beam, is considered positive if the scatterer approaches the radar.) From (1) - (3) follows the well-known formula for the response of the SAR to a point scatterer:

$$|a_{\text{SAR}}(t)|^2 \propto p_0^2 \left(\frac{\sin u}{u} \right)^2 \quad (4)$$

$$u = \frac{kV\Delta t}{R} \left(x_0 - Vt + \frac{R}{V} v_{\text{rad}} \right)$$

In fact, Eq. (4) contains the initial information on the formation of the SAR image of the ocean surface. As it can be seen, the image of a point scatterer is smearing along the azimuthal coordinate and, as a whole, shifts forward or backward in the direction of the SAR movement, depending on the sign of the radial component of the scatterer velocity. It can be said that all the features observed in the SAR image of the ocean result from the above effects, which are manifested taking into account the specifics of ocean waves.

The proposed method uses the fact that at small depression angle ψ the orbital velocity of the scatterer in projection onto the beams of two SARs has close values, but opposite signs: v_{rad} and $-v_{\text{rad}} + \Delta v_{\text{rad}}$. The difference Δv_{rad} is due to the fact that the orbital velocity has a

vertical component, and $\Delta v_{\text{rad}} \rightarrow 0$ when $\psi \rightarrow 0$. Thus, for two SARs we have

$$a_1(t') \propto p_0 \exp \left\{ i \left[\frac{k}{R} (x_0 - Vt')^2 - 2kv_{\text{rad}}t' \right] \right\} \quad (5)$$

$$a_2(t') \propto p_0 \exp \left\{ i \left[\frac{k}{R} (x_0 - Vt')^2 + 2k(v_{\text{rad}} - \Delta v_{\text{rad}})t' \right] \right\} \quad (6)$$

Let us write a_1 and a_2 in real form and then multiply them with each other:

$$a_1(t')a_2(t') \propto p_0^2 \cos \left[\frac{2k}{R} (x_0 - Vt')^2 - 2k\Delta v_{\text{rad}}t' \right] + p_0^2 \cos[2k(2v_{\text{rad}} - \Delta v_{\text{rad}})t'] \quad (7)$$

Let us apply the operation of matched filtering to the first term on the right-hand side of (7), having previously written it down in the usual complex form. For a system consisting of a pair of SARs taking into account the double frequency of the filtered signal we obtain:

$$|a_{\text{double SAR}}(t)|^2 \propto p_0^4 \left(\frac{\sin u}{u} \right)^2 \quad (8)$$

$$u = \frac{2kV\Delta t}{R} \left(x_0 - Vt + \frac{R}{V} \frac{\Delta v_{\text{rad}}}{2} \right)$$

Applying matched filtering to the second term in the right side of (7) gives a negligible value, which is natural due to the absence of a filtering object.

Comparing Eqns.(4) and (8), we immediately notice the following. First, the azimuthal resolution of a system of two SARs turns out to be two times higher than that of a conventional SAR, which has the same operating frequency and integration time. Second, that is most important, the effect of the orbital velocity of the scatterer decreases with decreasing depression angle and potentially can be brought to an insignificant.

As shown in the theory [1] in relation to traditional SAR, a shift in the image of a point scatterer means the same shift in the image of an element of the ocean surface, and the condition

$$\frac{R}{V} \sigma(v_{\text{rad}}) \leq \frac{\Lambda_v}{4|\cos\varphi|} \quad (9)$$

ensures that there is no superimposition of images of surface elements (see Introduction), i.e. no spectral cut-off (here, $\sigma(\Delta v_{\text{rad}})$ is the r.m.s. of radial velocity, Λ_v is the characteristic wavelength in the orbital velocity spectrum, and φ is the angle between the SAR flight direction and the general direction of ocean waves propagation).

Referring to Eqn. (8), we can write down a similar condition as

applied to the survey method under consideration:

$$\frac{R}{V} \sigma(\Delta v_{rad}) \leq \frac{\Lambda_v}{2|\cos\varphi|} \quad (10)$$

where $\sigma(\Delta v_{rad})$ is the r.m.s. of Δv_{rad} . A simple analysis showed that with the circular motion of the point scatterer both in the plane of incidence and in the plane perpendicular to it

$$\Delta v_{rad} = 2v_{orb} \cos \alpha \sin \psi \quad (11)$$

where α is the angle of deviation of the orbital velocity vector from the vertical. Having taken into account that

$$\frac{1}{2\pi} \int_0^{2\pi} \cos^2 \alpha \, d\alpha = \frac{1}{2} \quad (12)$$

we write down

$$\sigma(\Delta v_{rad}) = \sqrt{2} \sigma(v_{orb}) \sin \psi \quad (13)$$

whence the condition for the absence of spectral cut-off follows

$$\frac{R}{V} \leq \frac{\Lambda_v}{2\sqrt{2} \sigma(v_{orb}) \sin \psi |\cos \varphi|} \quad (14)$$

Thus, formula (14) is a criterion for the applicability of the considered method.

Note that it should be borne in mind that if for a conventional survey we consider the intensity of the SAR signal to be proportional to the surface elevations, then in this case the values of the obtained wave field turn out to be proportional to the square of the elevations.

So far, we have dealt with the image row exactly in the middle between two SARs. Obviously, for the formation of the swath, it is necessary to consider the case of an image row at a distance d from the middle one.

Consider the quantity

$$f(d) = \frac{1}{R_1} + \frac{1}{R_2}$$

Where R_1 and R_2 are slant ranges with respect to two SARs of a point offset by a distance d from the middle row, and

$$R_1^2 = R^2 + d^2 - 2Rd\cos\psi$$

$$R_2^2 = R^2 + d^2 + 2Rd\cos\psi$$

We rewrite $f(d)$ as

$$f(d) = \frac{1}{R} \left\{ \left[1 + \left(\frac{d}{R}\right)^2 - 2\frac{d}{R}\cos\psi \right]^{-1/2} + \left[1 + \left(\frac{d}{R}\right)^2 + 2\frac{d}{R}\cos\psi \right]^{-1/2} \right\} \quad (15)$$

and then express it through a series in powers of the small param-

eter d/R :

$$f(d) = \frac{2}{R} \left[1 + \sum_{n=1} b_n \left(\frac{d}{R}\right)^n \right] \quad (16)$$

Thus, for a row of the image spaced from the middle row at a distance d , we have:

$$a_{double\ SAR}(t) \propto \int_{t-\Delta t/2}^{t+\Delta t/2} dt' a_1(t') a_2(t') \exp \left[-i \frac{2k}{R} \left[1 + \sum_{n=1} b_n \left(\frac{d}{R}\right)^n \right] V^2 (t' - t)^2 \right] \quad (17)$$

The number of terms of the series taken into account is determined by the requirement

$$\left| \frac{2k}{R} b_n \left(\frac{d}{R}\right)^n (V\Delta t)^2 \right| \leq \frac{\pi}{4} \quad (18)$$

Having assumed $d=L/2$, where L is the swath width, one can determine the maximal number of terms, which should be taken into account. According to our calculation (see below), the first four terms of the power series with the coefficients

$$b_1 = 0, \quad b_2 = 3 \cos^2 \psi - 1, \quad b_3 = -2.5 \cos^2 \psi, \quad b_4 = 0.75 - 1.75 \cos^2 \psi$$

turned out to be sufficient to form a swath 100 km wide from space from an altitude of 400 km.

Numerical Estimates of the Conditions of Applicability of the Method

In order to understand which sensing scheme can be applied for this method, some evaluations have been performed. As the initial data, we took H - the flight altitude of the SAR carrier and ψ the depressing angle of the probe beam near the ocean surface. Then, taking into account the sphericity of the Earth, for the incidence angle ϑ and the slant range R we obtain

$$\sin \vartheta = \frac{a}{a+H} \cos \psi, \quad R = a \frac{\cos(\psi + \vartheta)}{\sin \vartheta} \quad (19)$$

where $a = 6371 \text{ km}$ is the Earth radius and ϑ is the incidence angle. The estimates were carried out for $\psi=30^\circ$ and the SAR carrier speed $V=8 \text{ km/s}$. For $H=400 \text{ km}$ (low near-earth orbit), we get $\vartheta=54.57^\circ$, $R=740 \text{ km}$ and $R/V=92.5\text{s}$. For $H=800 \text{ km}$, we get $\vartheta=50.30^\circ$, $R=1396 \text{ km}$, $R/V=174.5\text{s}$. For aircraft version we assume $H=10 \text{ km}$ and $V=1000 \text{ km/h}$, and get $\vartheta=59.84^\circ$, $R=20.3 \text{ km}$, $R/V=72.5\text{s}$.

We now need to evaluate the right side of (14), which we will perform by taking the near-surface wind speed $U=10 \text{ m/s}$. According to the simulation results given in [2], in this case $\Lambda_v \approx 70\text{m}$, while the Pearson-Moskowitz spectrum implies $\sigma(v_{orb}) \approx 0.68 \text{ m/s}$. Consequently, the right-hand side of (14) can be estimated as $(73/|\cos \varphi|) \text{ s}$, from which it follows that condition (14) is satisfied in the case of airborne SAR for any direction of waves propagation, but

in cases of space SARs, it is satisfied only at a sufficiently large angle φ .

However, the space options should not be rejected. The fact is that in the case of traditional survey the number of superimpositions is nothing more than the number of intersections of the straight-line $u(x)=Vt-x$ and the random curve $(R/V) v_{rad}(x)$ which, as can be seen from the geometry, is odd, i.e. the case of double superimposition is not realized. Evidently, the same takes place in considered case for the random curve $(R/V) (\Delta v_{rad}(x)/2)$. So the right-hand side of criterion (14) can be doubled and then the applicability condition is satisfied for the case of low orbit at any angle φ , and for the higher orbit on a not very limited interval of φ .

Now let's return to the issue of swath formation. We take $\lambda=5cm$, $\Delta t=1s$, $L=100km$ and evaluate the left part of (18) at $n = 4$. Then, for the case $H=400 km$, we obtain

$$\left| \frac{2k}{R} b_4 \left(\frac{L}{2R} \right)^4 (V\Delta t)^2 \right| = 0.25 \quad (20)$$

Consequently, when forming an image in the $L=100 km$ swath from a low and, moreover, from a higher orbit, it is possible to restrict the series in Eqn. (17) by the term $n = 4$. Having chosen a suitable swath, it is not difficult to obtain a similar estimate for the aircraft version.

Finally, the following should be noted. Strictly speaking, when discussing the criterion of applicability of the method, a modified formula (11) should be considered, namely

$$\Delta v_{rad} = 2v_{orb} \cos \left(\alpha + \frac{\psi_1 - \psi_2}{2} \right) \sin \frac{\psi_1 + \psi_2}{2} \quad (21)$$

or

$$\Delta v_{rad} = 2v_{orb} \cos \alpha \cos \frac{\psi_1 - \psi_2}{2} \sin \frac{\psi_1 + \psi_2}{2} \quad (22)$$

where ψ_1 and ψ_2 are the depression angles of the beams of two SARs for an arbitrary row of the image. Equation (21) refers to the case of circular motion of a point scatterer in the plane of incidence, and (22) to the case of a plane perpendicular to it. Applying the above estimates to the case of a low orbit and the edge row of a 100 km wide swath, we found $\psi_1 = 32.05^\circ$ and $\psi_2 = 28.17^\circ$. Due to the small difference ψ_1 and ψ_2 from $\psi = 30^\circ$, the difference between Eqns. (11), (21), and (22) can be considered insignificant.

Summary

Thus, the considered sounding method promises to provide a practically undistorted wave pattern with an increased resolution. Since the fundamental feature of the method is the use of low depressing angles, vertical polarization of radiation is preferable.

Indeed, the initial tests should be carried out using airborne SARs. The effectiveness of the method can be easily verified by comparing the image spectra obtained by each individual SAR on one side and the dual SARs system on the other.

References

1. K Hasselmann and S Hasselmann (1991) On the nonlinear mapping of an ocean wave spectrum into a synthetic aperture radar image spectrum and its inversion. *J Geophys Res C* 96:10713-10729.
2. M Kanevsky (2008) Radar imaging of the ocean waves. Elsevier, Oxford-Amsterdam, 206 p.
3. M Kanevsky (2020) Waves and noise in SAR imagery of the ocean. DOI:10.13140/RG.2.2.24416.71687
4. W Shao, Z Zang, X Li, and H Li (2016) Ocean wave parameters retrieval from Sentinel-1 SAR imagery. *Remote Sens* 8: 707.
5. L Ren, J Jang, G Zheng, J Wang (2015) Significant wave height estimation using azimuth cutoff of C-band RADAR-SAT-2 single-polarization SAR images. *Acta Oceanologica Sinica. English Edition* 34: 93-101.
6. M Kanevsky (2021) How to obtain a SAR image of the ocean surface that is actually free from the impact of orbital velocities. *J Mari Sci Res and Ocean* 4: 220-221.

Copyright: ©2021 Mikhail B Kanevsky. This is an open-access article distributed under the terms of the Creative Commons Attribution License, which permits unrestricted use, distribution, and reproduction in any medium, provided the original author and source are credited.